NRIAG Journal of Astronomy and Geophysics (2015) 4, 32–43

National Research Institute of Astronomy and Geophysics

NRIAG Journal of Astronomy and Geophysics

www.elsevier.com/locate/nrjag

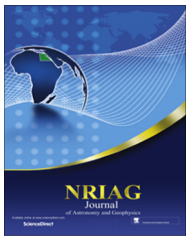

Paleo-tectonic positions of Northeast Africa during Cretaceous–Paleocene: Paleomagnetic study on East Gilf Kebir Plateau basalts [59 Ma], Southwestern Desert, Egypt

Hamza I. Lotfy [a,*], **Hatem H. Odah** [b]

[a] *Faculty of Science, Minia University, Minia 61519, Egypt*
[b] *National Research Institute of Astronomy and Geophysics (NRIAG), Egypt*

Received 19 January 2015; revised 25 February 2015; accepted 26 February 2015
Available online 20 March 2015

KEYWORDS

Paleomagnetism;
Paleo-latitude;
Western Desert of Egypt;
Alkali basalt;
Late Paleocene;
Selandian/thanetian

Abstract The middle/late Paleocene basalts which cover the Late Cretaceous sandstone in the East Gilf Kebir Plateau were sampled for paleomagnetic investigation. The progressive thermal demagnetization revealed that

- The hematite component was parallel to the present-day field and the goethite overprint. Its pole is considered as representing recent low-temperature martitization of the magnetite upon exposure to intensive chemical alteration.
- The magnetite-anchored component was N–S dual-polarity with shallow equatorial inclinations. Based on its overwhelming existence, this component was considered as the characteristic remanence of the sampled basalt. Its north pole (71.7°N/203.5°E) was considered as representing the geomagnetic field during the eruption of the basalt.

The reliability of the East Gilf Kebir basalt (59 ± 1.7 Ma) pole was constrained by its comparison with synchronous poles rotated from the main tectonic units using Euler Pole rotation. This basalt pole places NE Africa, along its present N–S azimuth at a far south tropical paleo-latitude. Cairo [30°N], was at paleo-latitude 11.8°N in middle/late Paleocene (59 Ma), that is about 18° south to its present-day latitude.

* Corresponding author.
E-mail address: Hiloutfy@yahoo.com (H.I. Lotfy).

Peer review under responsibility of National Research Institute of Astronomy and Geophysics.

ELSEVIER Production and hosting by Elsevier

http://dx.doi.org/10.1016/j.nrjag.2015.02.002

Comparing the present pole with the Mansouri ring complex (132 ± 10 Ma) Early Cretaceous pole (47°N/259°E) and two poles from the Wadi Natash volcanic field; the alkali basalt (104 ± 7 Ma) Middle Cretaceous pole [55°N/250°E] and the trachyte/Phonolite (86–78 Ma) Late Cretaceous pole [66.5°N/229°E], a Cretaceous–Paleocene segment [132–59 Ma] of the Apparent Polar Wander Path [APWP] of Africa could be traced. These poles can, concurrently, verify the paleo-azimuth and paleo-latitude evolution of the African plate during the Cretaceous and Paleocene.

1. Introduction

By the end of the Cretaceous, the Early Paleogene witnessed a major global plate reorganization associated with abrupt changes on the rotation poles of the main plates and the spreading centers of oceans. In the Atlantic domain, the rotation pole for South America and Africa changed abruptly and the spreading rate of the South Atlantic became very low (Cande et al., 1988; Nürnberg and Müller, 1991). This was, concurrently, associated with a change in the spreading direction in the Central Atlantic (De Klasz, 1978). Within the Neotethyan-Mediterranean domain, during the Paleogene, the continuing convergence between Africa and Eurasia remarkably slowed down (Dewey et al., 1989), and witnessed southward migration of the collisional fronts of the Taurides, Hellenides, Albinides and Dinarides orogenic belts in the Eastern Mediterranean region (Robertson and Grasso, 1995).

These global events had widespread temporal and spatial impacts in the structural evolution and the modes of deposition in Africa in general and its Northeastern part in particular. The first of these events was the termination of the Late Cretaceous compressional episodes which largely affected the northeast African-Arabian margin echoing a system of successive parallel lines of ENE-WSW faulted doubly-plunging anticlines known as "the Syrian Arc System" crossing NE Africa and extending to Levant. Then, during the Paleocene-early Eocene times, the sedimentary basins in North Africa and Egypt, recorded strong subsidence (Chatellier and Selvin, 1988), whereas the inter-basinal areas were affected by strike-slip faulting and folding episode (Isswai et al., 1999). This, apparently, extended southwards to the Central African Rift System and the Horn of Africa, developing the Mandera Fault Zone (Bosworth, 1992).

The echo of the Late Cretaceous-early Tertiary global tectonic events, was recorded in the Southwestern Desert of Egypt including the study area by widespread prolonged alkaline basaltic magmatism, which were, intensively, studied and mapped by the German researchers during the eighties of the Twentieth century covering almost all geological aspects (Berneau et al., 1986; Franz et al., 1987; Klitzsch, 1984; Klitzsch and Lejal-Nicol, 1984; Klitzsch et al., 1986–1987; Schandelmeier et al., 1983; Schandelmeier and Darbyshire, 1984; Schandelmeier et al., 1987; among others).

According to these authors, the study area, as a part of the Southwestern Desert of Egypt, lies in the western part of the East Sahara Craton, along what is called the Gebel Uweinat-Bir Safsaf-Aswan structural uplift. The widespread magmatism in this area, includes a wide spectrum of alkaline volcanics and subvolcanics extending from olivine basalts to trachyte-Phonolite-rhyolite suites, frequently, protruding through the Cretaceous sandstone plateau, and forming a prominent part of the exposed rock-units (Schandelmeier et al., 1987). These magmatic fields of extrusives and intrusives are referred to reactivated intra-plate fractures of the stabilized East Sahara Craton during the successive periods of re-adjustments of the African lithospheric plate. Volcanics of Permo-Triassic, Early Jurassic, Cretaceous and Tertiary age are found in form of volcanic plugs, sheets, and dykes within the volcanic fields protruding through the sandstone blanket in whole southwestern Desert.

The present paleomagnetic study was applied on the middle/late Paleocene alkali basalts (59 ± 1.7 Ma) (Franz et al., 1987) in three clusters in the subdued plateau east of the Gilf Kebir main plateau, to shed light on the paleo-tectonic position of Africa during the Early Tertiary global plate re-organization events, which were associated with the abrupt changes in poles of rotation of the main plates and changes in the spreading centers of oceans.

2. Geology and sampling

The study area lies in the Southwestern Desert of Egypt, east of the Gilf Kebir Plateau and west Bir-Safsaf area. It is a rectangle, extending between latitudes 23°–23°30′N and longitudes 27°–27°40′E, covering an area of about 3850 km^2 (Fig. 1).

The area is covered by two Middle Cretaceous Nubia-type sandstone units; the "Aptian" Abu Ballas formation made up of shallow-marine shale "Lingula Shale" intercalated with near-shore to coastal marine siltstone and fine-grained sandstone forming the lower slopes overlain by the Sabaya Formation (probably Albian) consisting mainly of medium- to coarse-grained cross-bedded flood-plain sandstone forming the top of the plateaus. Despite that both sandstones units are traceable in the field, they are grouped under "Cretaceous sandstone" in the geologic map (Fig. 1) simplified after Klitzsch et al. (1986–1987), to focus on the location of the alkali basalt clusters.

Within the study area, the East Gilf Kebir Plateau [EGKP] alkali olivine basalt, which is the sole magmatic rock-unit, is present in three separate clusters forming the heads of a triangle (Fig. 1). The eastern cluster includes circular and elongated volcanic plugs of variable diameters and altitudes associated with lava flows, whereas the southern includes a main ring dyke without flows, while the western cluster includes a large number of plugs associated with few flows. Pyroclastics are, generally, rare. Thermal effect is, obviously, observed in the structurally tilted sandstone, developing deep-red or even

black quartzite, in the vicinity of the protruding basalt plugs. It is worth mentioning that circular structural features are recorded throughout the area with or without basalt, and that many of the ferruginous blackish quartzite exposures, give a fake appearance of basalt which has a lighter gray color in natural exposures.

Microscopically, the EGKP basalt has two characteristic textures; the porphyritic texture is dominant in the lava flows and the coarse-grained texture in the plugs. However, the ring dyke in the southern cluster (Fig. 1) records both textures; coarse-grained texture in the inner cone and porphyritic in outer margin, both with the same mineral constituents (Franz et al., 1987). Chemically, the major and trace elements constituents of the basaltic rocks indicate that they are similar in the whole area. They are all typical within-plate basalt with a regional trend from low fractionation to west to high-fractionation to the east. This is reflected by the tendency of decreasing MgO and CaO and increasing Al_2O_3, Na_2O and K_2O trend from Uweinat eastwards to Aswan toward the plate margin (Franz et al., 1987). Being in the middle part of the Southwestern Desert the study areas are thus having median values of these elements between the two extremes.

The K/Ar whole rock age of the alkali olivine basalt in the study area is 59 ± 1.7 Ma (Franz et al., 1987). This age is along the boundary between the middle Paleocene (Selandian) and late Paleocene (Thanetian) which lies at 59.2 Ma, according to Gradstein et al. (2012) and Cohen et al. (2013) geologic timescales.

A number of twenty-four sites of the alkali olivine basalt distributed over the three basalt clusters in the study area, were collected for paleomagnetic study (Fig. 1). Due to the desert-weathering of the natural exposures, about thirty centimeters holes were dug to obtained fresh sharp-sided dark-black oriented blocks. Sampling was restricted to oriented blocks due to the shortage in water supply. A solar compass was exclusively used for orientation, as the effect of the local magnetic field of the basalt was noticeable on the magnetic compass.

3. Isothermal remanent magnetization [IRM]

The paleomagnetic measurements of the present research were carried on the Agico JR-6 dual-speed spinner magnetometer [sensitivity 2×10^{-3} mA/m], in the paleomagnetic laboratory of the National Research Institute of Astronomy and Geophysics [NRIAG] in Egypt. It included both the preliminary IRM study followed by the demagnetization of the natural remanence of the alkali basalt.

In order to classify the sampled sites according to their magnetic remanence carriers, one sample from each site was selected for isothermal remanent magnetization [IRM] study. The selected sample was progressively acquired isothermal remanence up to 800 mT. Twenty-five millitesla increments were adopted up to 150 mT, then wider increments of 50 mT followed by 100 mT till 800 mT. The acquired IRM was, then, stepwise thermally demagnetized till 680 °C or complete demagnetization. The demagnetization started with 50 °C increments to detect the contribution of secondary goethite as a remanence carrier, followed by wider increments in intermediate temperatures. Increments of 25 °C were retained at 550 °C while approaching the Curie temperature of magnetite [585 °C] and hematite [680 °C].

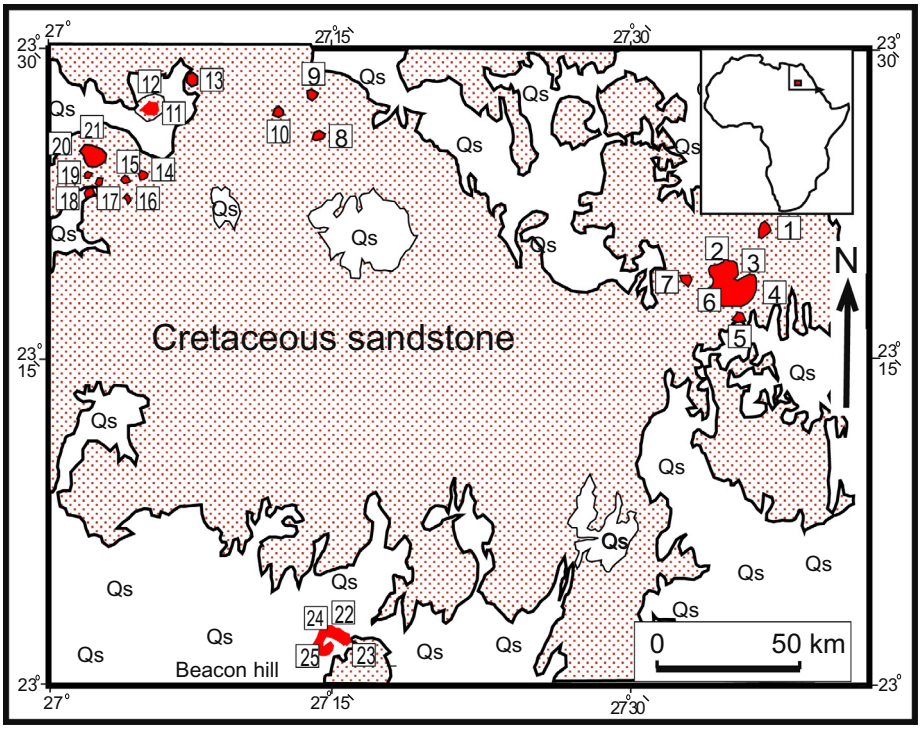

Figure 1 Geologic map of the study area in the Southwestern Desert of Egypt, simplified after Klitzsch et al. (1986–1987), showing alkali olivine basalt clusters. Qs denotes Quaternary wind-blown sand cover. Numbered squares represent the numbers and location of the sampling sites.

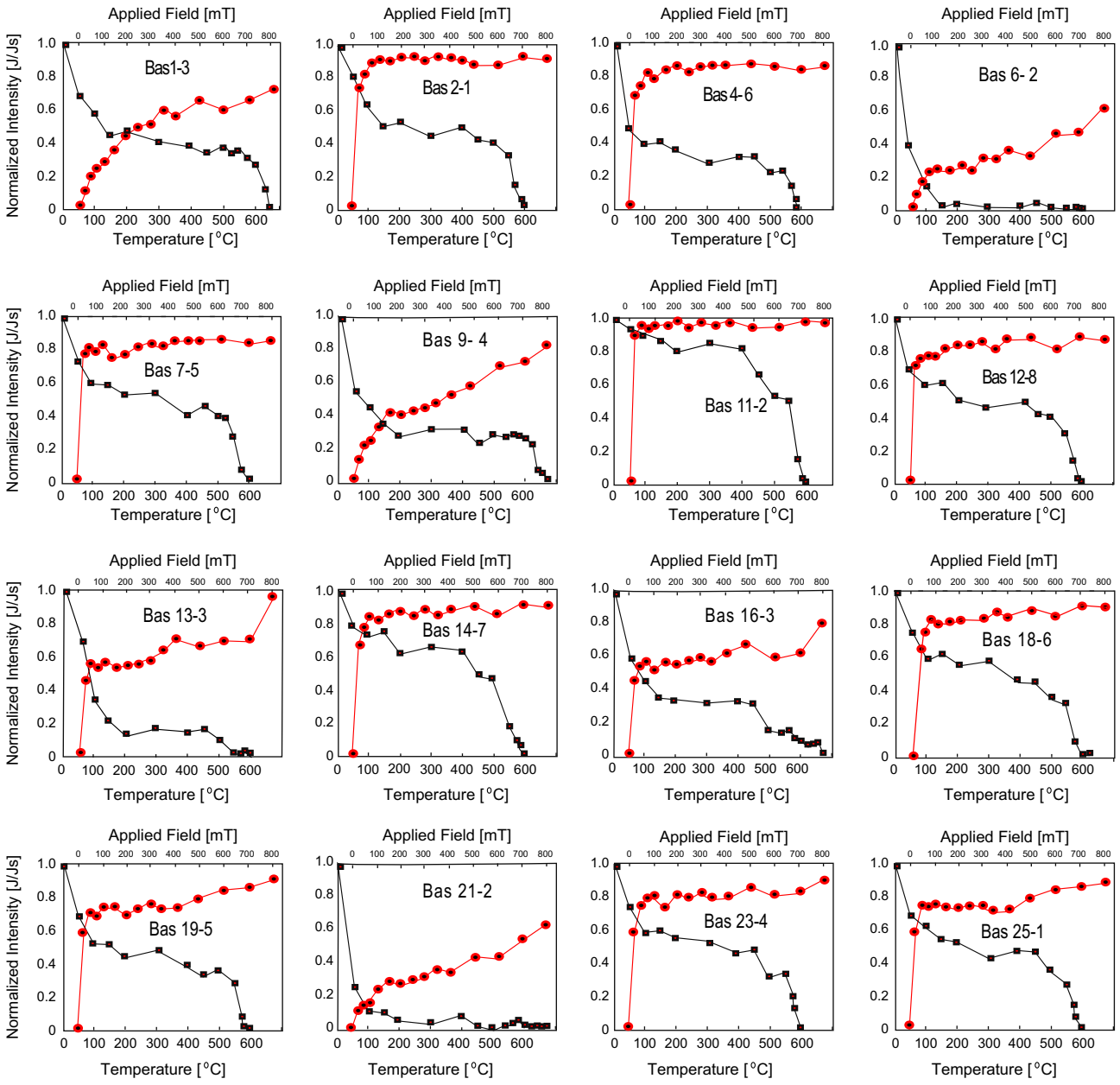

Figure 2 Isothermal Remanent Magnetization [IRM] curves of the olivine basalts. The ascending curves joining the circles are the normalized saturation magnetization intensity along the upper scale showing the applied saturating field up to 800 mT [note that the zero mT is not along the vertical scale to enhance the early ascending saturation of the magnetite]. The descending curves joining the squares are the normalized intensity decay during thermal demagnetization along the bottom scale showing temperatures (°C).

The inspection of IRM measurement revealed that most samples contain variable amounts of goethite contributing to their magnetic remanence (Fig. 2). This is reflected by the incomplete saturation of most samples up to 800 mT, followed by the sharp decay of their IRM upon thermal demagnetization temperature < 150 °C. This is observed in all samples in Fig. 2 except site Bas 11-2, which, apparently, does not contain goethite. Sites containing goethite as the sole remanence carrier, such as sites Bas 6-2 and Bas 21-2 (Fig. 2), were eliminated from the subsequent thermal demagnetization of their natural remanent magnetization [NRM] for paleomagnetic study.

The remaining sites were, then, classified into three groups: the magnetite-dominated, the hematite-dominated and the magnetite/hematite sites. Sites of the third group, such as site Bas 16-3 (Fig. 2), were also discarded from thermal demagnetization, due the expected complex unresolvable curved trajectories during the concurrent decay of their magnetite in the existence of the higher Curie temperature hematite.

However, the magnetite-dominated sites, which contained hematite as minor contributor, represent the majority of the sampled sites. These sites were characterized by rapid saturation upon acquiring an IRM < 100 mT, followed by almost

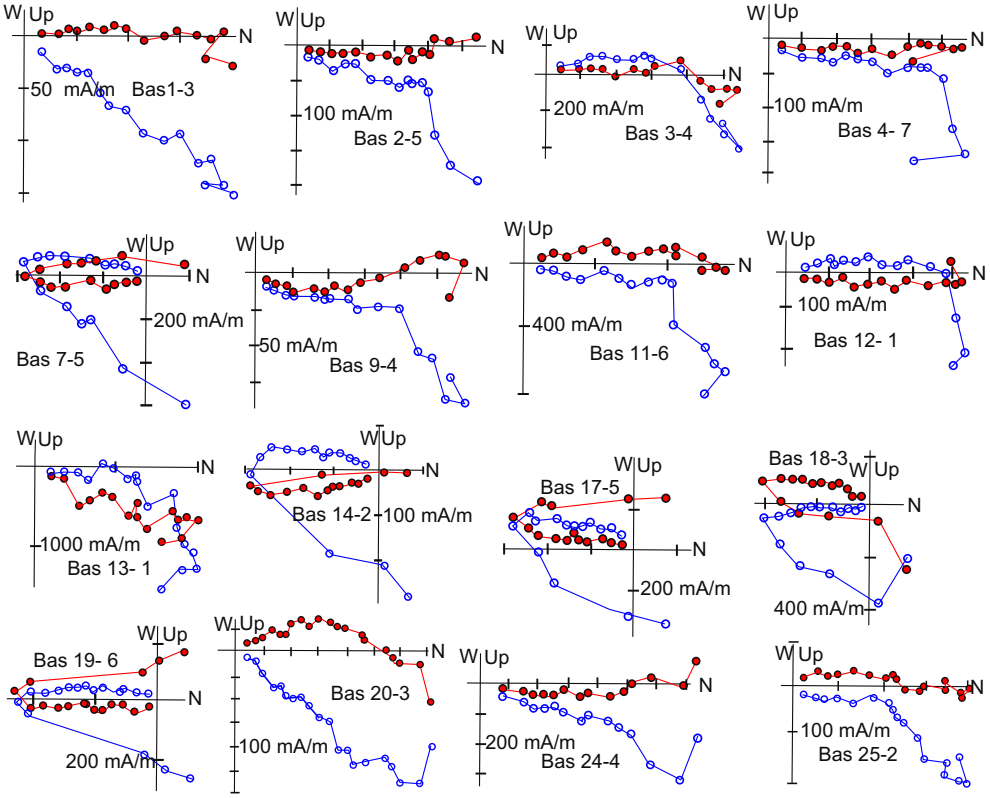

Figure 3 Orthogonal projections (Zijderveld, 1967) during progressive thermal demagnetization of the olivine basalt. Open circles (filled circles) denote the vertical (horizontal) projections.

complete thermal decay between 450 and 585 °C, such as site Bas 11-2, which was very fresh during sampling and contains magnetite as single remanence carrier. Most magnetite-dominated sites in Fig. 2 reflect the coexistence of secondary goethite and minor hematite, such as Bas 1-3, Bas 2-1, Bas 13-3 and Bas 18-6.

On the other hand, the hematite-dominated sites, of which site Bas 9-4 (Fig. 2) is an example, are never saturated up to 800 mT, then start decay at temperatures >600–680 °C. This group is represented by few partly-weathered brownish-colored sites. The coexistence of the goethite enhances the incomplete saturation of the IRM and complicates the thermal demagnetization pattern by a sharp early decay at temperature <150 °C.

4. Thermal demagnetization of the natural remanence

Each sample of both the magnetite-dominated and hematite-dominated sites was exposed to progressive stepwise thermal demagnetization up to 680 °C or until complete demagnetization. The increments were 50 °C up to 200 °C, then 100 °C steps, and become 25 °C above 550 °C.

Inspecting the decay trajectories in the orthogonal projections (Zijderveld, 1967) in Fig. 3, it was observed that most samples start with the early decay [<150 °C] of a soft northwards normal medium-inclination component residing in the goethite. Being parallel to the present-day field [PDF] in the study area, this component is considered as a PDF overprint. Then, the pattern of the decay of the natural remanence in both the magnetite-dominated and the hematite-dominated sites diverges:

1. In the hematite sites, after the early decay of the normal PDF, the trajectories retained their decay along the same direction swinging around the north with medium positive inclination until complete demagnetization at temperatures >600 °C, as in samples Bas 1-3, Bas 9-4, Bas 20-3 (Fig. 3). This obvious uni-vectorial decay along the PDF direction both the soft and the anchored components, reflects the low-temperature martitization of most primary magnetite in these samples in secondary martite, recording only PDF overprint.
2. The magnetite-dominated samples, on the other hand, were characterized by bi-vectorial decay. The early removal of the goethite PDF overprint was succeeded by change in trajectory direction. The anchored component, which decayed between 400 and 580 °C, was dual-polarity N–S with equatorial inclination swinging around zero, like most samples in Fig. 3.

Based on its dominant existence and residence in all magnetite sites (Fig. 3), the magnetite-anchored component was considered as the characteristic remanent magnetization of the EGKP olivine basalt in the study area. Its direction could represent the geomagnetic field during the eruption of these basalts in middle/late Paleocene [59 Ma].

5. Paleomagnetic means and poles

The straight demagnetization trajectories representing the isolated magnetic components was, then, visually delineated for at least three successive demagnetization steps in the orthogonal

Table 1 Paleomagnetic demagnetization results of East Gilf Kebir basalt [59 Ma], *N* = number of demagnetized samples/sites, *n* = number of isolated directions/site, PDF = present-day field overprint, Mag. Car. = Magnetic carrier, Dec. = declination [°], Inc, = inclination [°], *K* or (κ) = kappa precision parameter (Fisher, 1953), α95[°] = the semi-angle of the 95% cone of confidence about the paleomagnetic pole (Fisher, 1953), VGP [°N/°E] = Virtual geomagnetic north poles location, A95 = the semi-angle of the 95% cone of confidence about the paleomagnetic pole. Shaded sites are included in the hematite mean direction and paleomagnetic pole only as they are considered as present-day field overprint. Sites with [*] are not included in the anchored components means.

East Gilf Kebir Plateau [EGKP] Basalt [23.25°N/27.33°E] [59 ± 1.7 Ma]									
Demag. sites		Goethite component [PDF]			Anchored component				
Site	N	*n*	Dec.°/Inc.°	K/α95°	Mag. Car.	*n*	Dec.°/Inc.°	K/α95°	VGP [°N/°E]
Bas-1	5	3	3/57	22.8/26.5	Hematite	3	359/41	34/21.4	89/312.3
Bas-2	7	4	358/51	21.3/20.4	Magnetite	6	9/8	47.7/9.8	69/181.6
Bas-3	8	6	2/34	22.5/14.4	Magnetite	8	359/-5	46.3/11.4	64.2/209.6
Bas-4	8	5	7/57	15.8/19.9	Magnetite	7	5/18	49.3/8.7	75.2/187.7
Bas-7	6	4	356/34	16.1/23.6	Magnetite	6	177/-11	27.6/13	72/217
Bas-8	6	2	6/42	-/-	Hematite	6	11/39	23/14.3	80/122
Bas-9	5	3	351/17	23.2/26.6	Hematite	4	12/52	40/14.7	76/73
Bas-11	6	4	2/48	19.9/21.1	Magnetite	6	353/23	23/14	77/239
Bas-12	8	2	357/53	-/-	Magnetite	8	2/−2	24.5/11.4	65.7/202.5
Bas-13*	3	2	17/66	-/-	Magnetite	3	16/6	18/27	Wide α95
Bas-14	7	5	2/49	13.5/21.6	Magnetite	7	168/-15	20.2/13.7	70.6/245.7
Bas-17	8	5	353/27	18.2/18.5	Magnetite	7	190/-15	26/12.1	71.7/174.2
Bas-18	6	3	22/58	18.1/29.9	Magnetite	6	191/1	25.5/12	64/181.6
Bas-19	7	3	346/12	23/26.8	Magnetite	6	178/-3	27/13.1	68.2/212.7
Bas-20	8	5	9/61	29/14.4	Hematite	7	338/54	25/12.2	69/333
Bas-21*	5	3	3/18	26/24.8	No stable characteristic remanent magnetization				
Bas-23	6	2	3/51	-/-	Magnetite	6	4/10	22/14.6	71.4/195
Bas-24	4	4	351/28	17.7/22.5	Magnetite	4	9/27	47/13.5	77.6/162.2
Bas-25	5	4	9/27	31.2/16.7	Magnetite	7	351/5	32/13.7	67.5/231.4
	19/118	19/69	.5/42	21.2/7.5	Magnetite mean	13/84	1.2/9.8	47/6.3	71.7/203.5 κ = 80 A95 = 4.7°
					Hematite mean	4/20	1/47	40.3/14.6	84.6/35 κ = 32 A95 = 16.5°

(Zijderveld, 1967) projections (Fig. 3). The best-fit line of each component was determined using the principal component analysis [PCA] technique (Kirschvink, 1980). The site-means for both the soft [PDF] and the anchored [magnetite or hematite] remanence directions were, then, calculated with their associated statistical parameters; the precision parameter (*K*) and the semi-angle of the cone of 95% confidence (α95) (Fisher, 1953). Three separate overall rock-unit means were, then calculated for the soft PDF component and the two anchored components. At last, two separate paleomagnetic poles for the hematite and magnetite-residence components were located (Table 1; Fig. 4).

The individual directions and the site-means of both the soft PDF component residing in goethite and the anchored hematite components were all of normal polarity dispersed around the present-day field direction in the study area, yielding two overall means at (0.5°/42°) and (1°/47°), respectively. However, based on its presence in only four sites (20 samples) all having normal polarity grouped around the present-day field, the hematite component was considered as representing PDF overprint like the goethite component (Table 1; Fig. 4). This overprint was, apparently, acquired during the chemical alteration of the basalts by the ascending ferruginous solutions obliterating the primary magnetite and developing secondary martite in few sites upon their exposure to intensive alteration near fault planes. This chemical alteration by secondary ferruginous solutions is widely observed in the area developing reddish black sandstone hillocks.

On the other hand, the site-means of the magnetite anchored component were bipolar, N–S antipodal, with shallow inclination fluctuating around zero. The rock-unit mean direction of the magnetite component was (1.2°/9.8°). The normal polarity of the magnetite component was recorded in eight sites (Dec./Inc. = 1.5°/10.6°) with observed length of the vector resultant $R = 7.82$ and a precision parameter $K = 37.86$. On the other hand, the reversed polarity was recorded in five sites (Dec./Inc. = 180.8°/−8.7°) with $R = 4.91$ and $K = 45.94$. Accordingly, both the normal and reverse polarity sites of the magnetite anchored component share a common mean at the 95% confidence, and positively pass the reversal test of McFadden and Lowes (1981). This implies that the antipodal means of the magnetite component are clean from secondary overprints.

Based on its dominant existence and distinct delineation in thirteen sites (84 samples), bipolarity, divergence from PDF direction, and its positive reversal test, the anchored magnetite component could be considered the primary characteristic remanent magnetization [ChRM] of the EGKP basalt

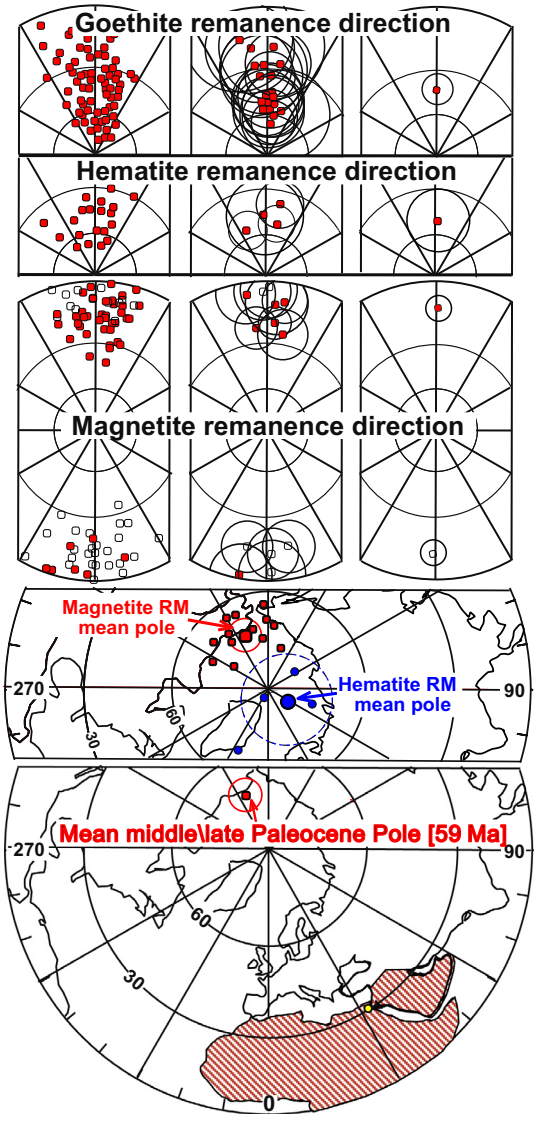

Figure 4 Equal area projections showing the directions of the isolated demagnetized magnetic components in East Gilf Kebir basalt. In the upper part, the samples-direction, site-means and rock-unit mean of the PDF overprint carried by goethite (< 150 °C). Next down, the directions, site-means and rock-unit mean of the anchored hematite remanence > 585 °C. Next, the directions, site-mean and rock-unit mean of the characteristic anchored magnetite (ChRM). The lower two projections represent the virtual geomagnetic poles [VGPs] of the site-means together with the mean paleomagnetic pole of both the hematite remanence (close to the axial geocentric dipole) and the magnetite ChRM remanence representing the middle/late Paleocene [59 Ma] paleomagnetic pole of East Gilf Kebir basalt, with their semi-angles of the cones of 95% confidence [A95].

(Table 1; Fig. 4). Therefore, the paleomagnetic pole of the magnetite component (71.7°N/203.5°E, κ = 80, A95 = 4.7°), could be considered as representing the geomagnetic field during the extrusion of the alkali olivine basalt in EGKP area during the middle/late Paleocene [59 Ma].

Table 2 The Euler pole rotation parameters used to rotate the paleomagnetic poles of the North American Craton, Stable Europe and Greenland to the African coordinates. All Euler poles parameters are interpolated at 59 Ma from the original rotation parameters.

Tectonic units rotated	Euler pole rotation parameters			Reference
	Latitude (°)	Longitude (°)	Angle (°)	
Stable Europe versus N. American Craton	56	145.56	−13.9	Gaina et al. (2002) Interpolated at 59 Ma.
Greenland versus N. American Craton	28.8	222.1	−3.86	Gaina et al., (in prep 2008) (in Torsvik et al., 2008) Interpolated at 59 Ma.
N. American Craton versus Africa	81.3	5.6	18.84	Müller et al. (1997) Interpolated at 59 Ma.

6. Discussion and comparison with tectonically rotated poles

In order to constrain the fidelity of the obtained paleomagnetic pole of the EGKP basalt to represent the geomagnetic pole of Africa in the middle/late Paleocene, its synchronous poles from Stable Europe, Greenland, and the North American Craton were rotated to the African coordinates using the Euler pole rotation. The rotation parameters were all interpolated to 59 Ma (Table 2), from the original published parameters. Reliable paleomagnetic poles with ages (59 ± 5 Ma) were selected from the global databases, comprehensive reviews and recent global reconstructions (McElhinny and Lock, 1996; Pisarevsky, 2005; Torsvik, 2008, 2012; Van der Voo, 1993). The EGKP basalt paleomagnetic pole is, further, compared with its coeval poles (60 Ma) of the recent Global Apparent Polar Wander Paths [APWPs] such as Torsvik et al. (2008, 2012) (Table 4).

Eleven paleomagnetic poles representing the Paleocene igneous rocks in western Stable Europe were selected and rotated to Africa (Table 3A). The rotation parameters of Gaina et al. (2002) were interpolated at 59 Ma (Table 2) between the rotation parameters of An-31y [68.737 Ma] and An-25y [55.904 Ma] and used to rotate the European poles to the North American coordinates. Subsequently, the rotation parameters of Müller et al. (1997) were interpolated at 59 Ma between An-25 [55.9 Ma] and An-30 [65.6 Ma] and used to rotate the rotated poles from North America to the African coordinates. The European poles rotated to the African coordinated are, generally, clustered around the EGKP basalt pole (71.7°N/203.5°E) (Fig. 5A). Both the mean European pole (73.7°N/209°E) and its A95 cone lie inside the A95 cone of the EGKP basalt pole (Fig. 5A).

Eleven poles from the Paleocene igneous rocks of Greenland were selected and rotated to Africa (Table 3B). The rotation parameters of Gaina et al. (2008, in Torsvik

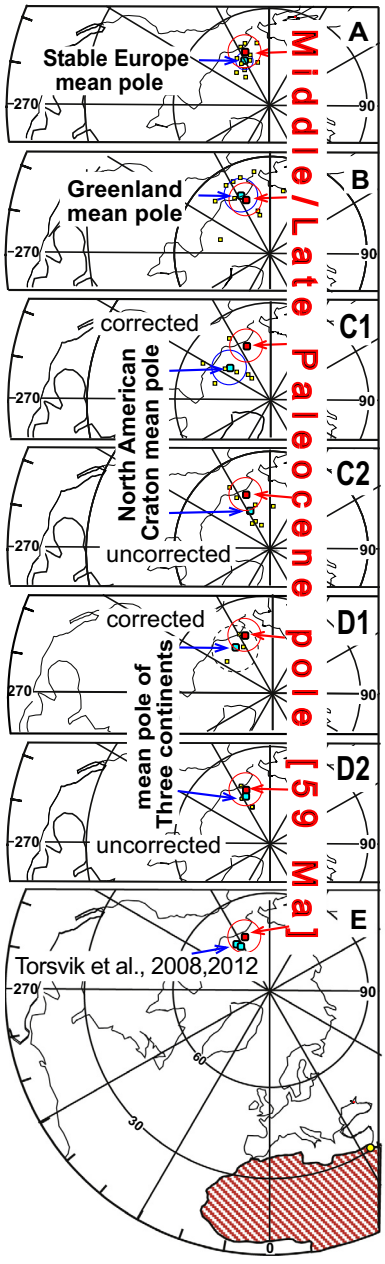

Figure 5 Comparison between the East Kilf Kebir basalt pole with paleomagnetic poles rotated from the main tectonic units to the African coordinates using Euler pole rotation. Mean paleomagnetic pole for each continent is presented with its semi-angle of the cone of 95% confidence [A95].

et al., 2008), were interpolated at 59 Ma between An-25y [55.904 Ma] and An-31y [68.737 Ma] (Table 2) and used to rotate the Greenland poles to the North American coordinates. Then, the rotation parameters of Müller et al. (1997) interpolated at 59 Ma are used to rotate these poles to the African coordinates. The rotated Greenland poles are scattered around the EGKP basalt pole (Fig. 5B). The Greenland mean pole (70.1°N/206.6°E) lies very close to the pole of the present study with their A95 cones largely overlapping (Fig. 5B).

Seven poles representing the North American Craton were selected, three of them are from sedimentary rocks (Table 3C). The rotation parameters of Müller et al. (1997) interpolated at 59 Ma are used to rotate the North American Craton poles to the African coordinates (Table 2). Two mean poles were calculated for the North America Craton, one without applying inclination-shallowing correction for sedimentary poles (77°N/210°E] and the other with correction (74°N/230°E] (Table 3C). It was, obviously, observed that the corrected poles are of somewhat dispersed and their mean pole lies at a much higher longitude with respect to the mean poles rotated from Stable Europe and Greenland as well as the pole of the present study (Table 4, Fig. 5C1). On the other hand, the uncorrected poles are better grouped and their mean lies much closer to the rotated poles of Stable Europe, Greenland and the pole of EGKP basalt (Table 4, Fig. 5C2).

In order to further constrain the paleomagnetic pole of the EGKP basalt, it was compared with the mean pole of the main continents; the Stable Europe, Greenland and the North American. Two mean poles are calculated, one with the American poles corrected for inclination shallowing (Fig. 5D1) and the other without correction (Fig. 5D2). The first mean lies at a higher longitude with its semi-angle of the cone of 95% confidence (A95) partially overlapping with that of the present pole (Fig. 5D1). On the other hand, the second mean lies very close to the EGKP basalt (Fig. 5D2).

The present EGKP basalt pole was, also, compared with synchronous poles [60 Ma] from some recent Global Apparent Polar Wander Paths (Torsvik et al., 2008, 2012) (Table 4). It is quite evident that the two poles of the APWPs are in reasonable accordance with the EGKP basalt pole which lies at somewhat lower longitude (Table 4, Fig. 5E).

7. Conclusions and Cretaceous–Paleocene Paleotectonic motion of Africa

Comparing the present middle/late Paleocene paleomagnetic pole of the EGKP basalt [59 ± 1.7 Ma] which lies at (71.7°N/203.5°E) with the Mansouri ring complex [132 ± 10 Ma, Early Cretaceous] pole at (47°N/259°E) (Lotfy, 2015) and the two poles from the Wadi Natash alkaline volcanic field; the alkali basalt [104 ± 7 Ma, Albian] Middle Cretaceous pole (55°N/250°E) and the trachyte/Phonolite [86–78 Ma, Late Cretaceous] pole (66.5°N/229°E) (Lotfy, 2011), a Cretaceous-Paleocene segment [132–59 Ma] of the Apparent Polar Wander Path [APWP] of Africa was traced (Fig. 6). When compared with the Coeval segment of the Global Apparent Polar Wander Path [130–80 Ma] of Torsvik et al. (2008, 2012), the two segments show reasonable resemblance (Fig. 6) with the present segment showing a little lower latitudes. However, it can be noticed that the paleomagnetic pole of Wadi Natash alkali basalt (104 Ma) projects between the two poles [100, 110 Ma] of Torsvik et al. (2008, 2012) but still at lower latitude (Fig. 6).

The four aforementioned Egyptian paleomagnetic poles can, concurrently, be used to verify the paleo-azimuth and paleo-latitude evolution of the African Plate during the Cretaceous and Paleocene time (Fig. 6). The Mansouri ring Complex [132 Ma] pole places the African plate about 31° clockwise to the present-day geocentric axial dipole with Cairo [now at 31°N] at 1.5°S paleo-latitude (Fig. 6). During

Table 3A Middle/late Paleocene paleomagnetic North poles [59 ± 5 Ma] of Stable Europe rotated to the African coordinates using Euler pole rotations parameters (Table 2). K/A95 denotes the precision parameter and the semi-angle of the 95% cone of confidence about the pole (Fisher, 1953).

Rock-unit	Age	K/A95 (°)	North Pole (°N/°E)	Africa (°N/°E)	References
Vaternish dyke swarm, Scotland	59	21/3.5	76/160	72.8/202.6	Wilson et al. (1974)
Arran dykes, Scotland	59.4	37/1.2	81.7/180	75/226	Dagley et al. (1978)
Arran intr. and extr.	59.5	-/2.8	80/160	76/212.6	Hodgson et al. (1990)
Sleat dikes, Scotland	59.8	/1.5	82.5/158	77.5./220	Wilson et al. (1982)
Skye lavas, Scotland	59.8	/2.5	77.7/145.4	76.4/197.3	S. Rousse 2011 per. Com. (Torsvik 2012)
Ardnamurchan cplx, Scotland	60	-/2.7	77/175	71.7/214	Dagley et al. (1984)
Faroe Islands flood volcs., Denmark	60.1	24.5/4.5	71.4/154.7	70/190.7	Riisager et al. (2002)
Rhum and Canna igneous, Scotland	60.7	33.5/2.6	81/179	74.5/224	Dagley and Mussett (1981)
Mull Lava, Scotland	60.9	-/4.7	73/166	69.5/201.6	Ganerød et al. (2008)
Antrim lavas basalt, Ireland	61	–/4.7	79/167	74.3/213.5	Ganerød et al. (2010)
Muck and Eigg Ig.	61.2	21.5/2.7	74/171	69.6/206	Dagley and Mussett (1986)
Mean of Stable Europe [N = 11 poles]	**m/l Paleoc.**	**358/2.4**		**73.7/209**	

North pole represents the paleomagnetic pole position after the original author(s), while **Africa** represents the "Stable Europe" poles in the previous column after being rotated (using the Euler Poles) to become representing Africa by the authors o this article.

Table 3B Middle/late Paleocene paleomagnetic North poles [59 ± 5 Ma] of Greenland rotated to the African coordinates using Euler pole rotations parameters (Table 2).

Rock-unit	Age	K/A95 (°)	North Pole (°N/°E)	Africa (°N/°E)	Reference
Nuussuaq lava, Kanisut mb	55	11/10.3	74.6/159.4	77.8/196	Riisager et al. (2003b)
Kangerdlugsuaq dykes, Irminga	54.5	-/6	63/180	64.7/208	Faller and Soper (1979)
Scoresby Sund lava	55	-/15	63/174	65.3/202	Tarling (1967)
Skaergaard intrusion	55.5	40/4.2	61/165	64/191	Schwarz et al. (1979)
Kangerdlugssuaq basalt	55.5	105/9	63.4/185	64.5/213.5	Faller (1975)
Jacobsen Fjord dykes	59	69/3.7	68/178	69.8/209	Faller and Soper (1979)
Jacobsen Fjord basalt	59.5	-/9	64/184.5	65.3/213	Faller and Soper (1979)
Disko Island Lava comb.	60.5	-/3.2	67.5/195	67.7/226	Athaval and Sharma (1975)
Svartenhuk lavas, Vaigat Fm.	60 ± .5	25/9.8	76.2/218	73.6/254	Riisager et al. (2003b)
Nuussuaq and Disko lava, Vaigat Fm.	60 ± .5	20/9.1	64.8/141.5	69.8/166	Riisager et al. (2003a)
West Greenland comb.	58	-/6.2	73.6/160.5	76.8/195.5	Riisager et al. (2003a)
Mean of Greenland [N = 11 poles]	**M/L Paleoc.**	**84.8/5**		**70.1/206.5**	

North pole represents the paleomagnetic pole position after the original author(s), while **Africa** represents the "Stable Europe" poles in the previous column after being rotated (using the Euler Poles) to become representing Africa by the authors o this article.

Table 3C Middle/late Paleocene paleomagnetic North poles [59 ± 5 Ma] of the North America Craton rotated to the African coordinates using Euler pole rotations parameters (Table 2). Bracket poles of sedimentary rocks are poles without inclination shallowing correction. In the bracket mean pole and statistical parameters, the sedimentary poles are used without inclination correction.

Rock-unit	Age	K/A95 (°)	North Pole (°N/°E)	Africa (°N/°E)	Reference
Bighorn Basin	55	—/4.4	(81.4/168) 74/228.8	(81.5/205) 72/252	Clyde et al. (2007)
Rhyolite intrusion and contact, Co	57 ± 7	76/14	68/189	67/214	McMahon and Strangway (1968)
Nacimiento Fm. NM.	60–65	-/3	(76/146.5) 75/204.7	(77/176) 73.5/232	Butler and Taylor (1978)
Gringo Gulch Volcs, Az.	63 ± 2	678/1.1	77/201	75.6/229.7	Vugteveen et al. (1981)
Edmonston Gp., Alberta, Ca	63	24/6.6	(72/185) 68/218	(71.5/212) 66/241	Lerbeckmo and Coulter (1985)
Comb. Paleocene intrusions, Mo	63 ± 4	43/3.7	82/170.6	81/209	Diehl et al. (1983)
Alkalic intrusions, Mo	64 ± 3	41/3.9	80.5/179	80/214.5	Jacobson et al. (1980)
Mean of the North American Craton [N = 7 poles]	**m./l. Paleoc.**	**(147/5) 119/5.5**		**(77/210) 74/230**	

North pole represents the paleomagnetic pole position after the original author(s), while **Africa** represents the "Stable Europe" poles in the previous column after being rotated (using the Euler Poles) to become representing Africa by the authors o this article.

Table 4 The middle/late Paleocene paleomagnetic North Pole of the African Plate of the East Gilf Kebir basalt Ring. B. The mean poles [59 ± 5 Ma] rotated from the main tectonic units with the overall mean of the three continents rotated to the African coordinates. C. Mean middle/late Paleocene [60 Ma] poles from recently calculated Global Apparent Polar Wander Paths [APWP] rotated to the African coordinates. [K/A95] denotes the precision parameter and the semi-angle of the 95% cone of confidence around the mean pole. Cairo Ref. and Plat. denote the corresponding paleo-declination, paleo-inclination and paleo-latitude predicted at the reference location of Cairo, Egypt [30°N/31°E] from the cited poles.

A	Present study	Age (Ma)	Sites	Pole (°N/°E) [Africa]	K/A95 (°)	Cairo Ref. [Dec.°/Inc.°]	Plat. (°)
1	**Gilf Kebir basalt [23.25°N/27.33°E]**	**59 ± 1.7 Ma**	**13**	**71.7N/203.5E**	**80/4.7**	**2.4/22.7**	**11.8**
B	Tectonic Unit	Age (Ma)	N	Mean pole (°N/°E) [Africa]	K/A95)(°)		
1	North American Craton	59 ± 5	7	77/210 Uncorrected	147/5	0/31	16.5
				74/231 Corrected	119/5.5	355/28	14.9
2	Stable Europe	59 ± 5	11	73.7/209	355/2.4	.6/26	13.5
3	Greenland	59 ± 5	11	70.1/206.6	84.8/5	1.5/19.7	10.1
	Mean of three continents1	59 ± 5	3	73.6/208 Uncorrected	525/5.4	1/25.8	13.5
	Mean of three continents 2	59 ± 5	3	73/214.6 Corrected	322/6.9	359/24.8	13
C	Global APWP	Age [Ma]	N	**Mean pole (°N/°E) [Africa]**	A95[°]		
1	Global APWP (Torsvik et al., 2008) rotated to African coordinate	60	30	**74.3/213.5**	2.4	359.3/27	14.3
2	Global APWP (Torsvik et al., 2012) rotated to African coordinate	60	44	**72.9/215.3**	2.1	358.7/24.5	12.8

North pole represents the paleomagnetic pole position after the original author(s), while **Africa** represents the "Stable Europe" poles in the previous column after being rotated (using the Euler Poles) to become representing Africa by the authors o this article.

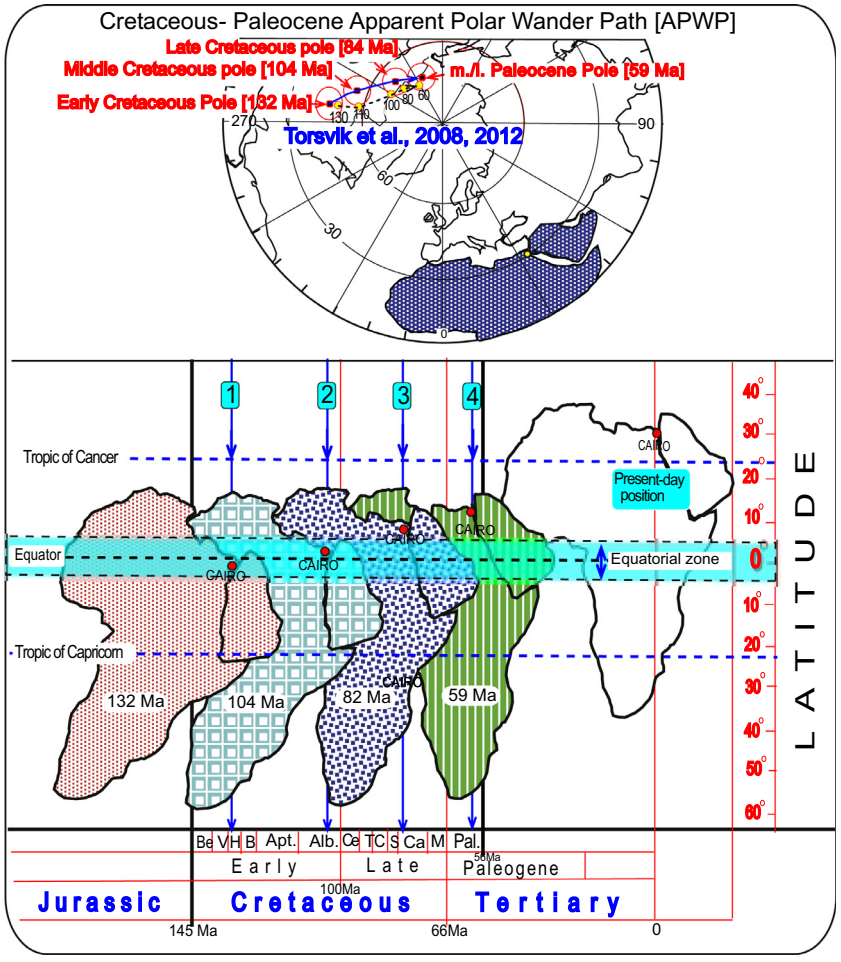

Figure 6 Four paleomagnetic poles from Egypt plotted on equal area projection; the Mansouri ring complex (132 Ma), the Wadi Natash field basalt (104 Ma) and Trachyte/Phonolite (86–78 Ma) and the East Gilf Kebir alkali basalt (59 Ma), compared to the 130–60 Ma segment of the Global Apparent Polar wander Path (Torsvik et al., 2008, 2012) in the African coordinates. Lower part, four successive paleotectonic positions of Africa based on the aforementioned paleomagnetic poles.

the eruption of the alkali basalt of Wadi Natash [104 Ma, Albian], Africa became about 20° clockwise and Cairo reached paleo-latitude 1.5°N. By the Late Cretaceous, when the Trachyte/Phonolite plugs and ring dykes of Wadi Natash were emplaced [86–78 Ma], Africa became 6° clockwise with Cairo at 7.5°N. Finally, during the eruption of the middle/late Paleocene, the EGKP alkali basalt of the present study in the Southwestern of Egypt, Africa became almost along the present-day azimuth (or about 2° counterclockwise), with reached the paleo-latitude of Cairo reaching 12°N (Fig. 6).

Therefore, it can be concluded that between the Early Cretaceous [132 Ma, Hauterivian] and the middle/late Paleocene [59 Ma, Selandian/Thanetian], Africa has been rotating counterclockwise 33° and concurrently translating northwards about 13.5° of latitudes (Fig. 6). During the three time segments, both the rates of counterclockwise rotation and northwards translation varies as well as the relative contribution of rotation with respect to translation. Furthermore, Northeast Africa, apparently, remained Equatorial for most of the Cretaceous and moved north of the equatorial zone during the Late Cretaceous (Fig. 6).

Acknowledgements

We would like to express my deepest gratitude and sincere thanks with appreciation to Prof. Dr. Esmat Abd El-All. Chairman of the department of Geomagnetism and Geoelectricity, for her crucial role and willing support during the progress of this research. We are, also, grateful to all my colleagues and staff members in the Geomagnetism Laboratory, for offering their inspired support during the progress of this research. This research was supported by the official research funds of the Minia University, Minia, Egypt, given to the Faculty members at the Faculty of Science. Sincere thanks are all due to the anonymous reviewers of these papers, whose specific and insightful comments and suggestions greatly improved the manuscript.

References

Athavale, R.N., Sharma, P.V., 1975. Paleomagnetic results on Early Tertiary lava flows from West Greenland and their bearing in the evolution history of the Baffin Bay-Labrador Sea region. Can. J. Earth Sci. 12, 1–18.

Berneau, R., Darbyshire, D.P.F., Franz, G., Harms, U., Huth, A., Mansour, N., Pasteels, P., Schandelmeier, H., 1986. Petrology, geochemistry and structural development of the Bir Safsaf-Aswan uplift, Southern Egypt. J. Afr. Earth Sci. 6, 79–90.

Bosworth, W., 1992. Mesozoic and Early Tertiary rift tectonics in East Africa. In: Ebinger, C.J., et al. (Eds.) Seismology and related sciences in Africa. Tectonophysics. Special volume 209, pp. 115–137.

Butler, R.F., Taylor, L.H., 1978. A middle Paleocene paleomagnetic pole from the Nacimiento formation, San Juan Basin, New Mexico. Geology 6, 495–498.

Cande, S.C., LaBrecque, J.L., Haxby, W.F., 1988. Plate kinematics of the South Atlantic: Chron C34 to present. J. Geophys. Res. 93, 13479–13492.

Chatellier, J.Y., Selvin, A., 1988. Review of African petroleum and gas deposits. J. Afr. Earth Sci. 7, 561–578.

Clyde, W.C., Hamzi, W., Finarelli, J.A., Wing, S.L., Schankler, D., Chew, A., 2007. Basin-wide magnetostratigraphic framework for the Bighorn Basin, Wyoming. Geol. Soc. Am. Bull. 119, 848–859.

Cohen, K.M., Finney, S.C., Gibbard, P.L., Fan, J.-X., 2013. The ICS international chronostratigraphic chart. Episodes 36, 199–204.

Dagley, P., Mussett, A.E., 1981. Palaeomagnetism of the British Tertiary igneous province: Rhum and Canna. Geophys. J. Roy. Astron. Soc. 65, 475–491.

Dagley, P., Mussett, A.E., 1986. Palaeomagnetism and radiometric dating of the British Tertiary igneous province: muck and Eigg. Geophys. J. Roy. Astron. Soc. 85, 221–242.

Dagley, P., Mussett, A.E., Wilson, R.L., Hall, J.M., 1978. The British Tertiary igneous province: palaeomagnetism of the Arran dykes. Geophys. J. Roy. Astron. Soc. 54, 75–91.

Dagley, P., Mussett, A.E., Skelhorn, R.R., 1984. Palaeomagnetism of the Tertiary igneous complex of Ardnamurchan. Geophys. J. Roy. Astron. Soc. 79, 911–922.

De Klasz, I., 1978. The West African sedimentary basins. In: Moullad, A.M., Nairn, A.E.M. (Eds.), The Phanerozoic Geology of the World: The Mesozoic. Elsevier, Amsterdam, Netherlands, pp. 371–399.

Dewey, J.F., Helman, M.L., Turco, E., Hutton, D.H.W., Knott, S.D., 1989. Kinematics of the western Mediterranean. In: Coward, M.P., Dietrich, D., Park, R.G. (Eds.) Alpine tectonics. Geological Society [London]. Special publication 45, pp. 265–283.

Diehl, J.F., Beck, M.E., Beske-Diehl, S., Jacobson, D., Hearn, B.C., 1983. Paleomagnetism of the late Cretaceous- Early Tertiary North-Central Montana Alkalic Province. J. Geophys. Res. 88, 10593–10609.

Faller, A.M., 1975. Palaeomagnetism of the oldest Tertiary basalts in the Kangerdlugssuaq area of East Greenland. Bull. Geol. Soc. Denmark 24, 173–178.

Faller, A.M., Soper, N.J., 1979. Palaeomagnetic evidence for the origin of the coastal flexure and dyke swarm in central E. Greenland. J. Geol. Soc. Lond. 136, 737–744.

Fisher, R.A., 1953. Dispersion on a sphere. Proc. R. Soc. Lond. A217, 295–305.

Franz, G., Puchelt, H., Pasteels, P., 1987. Petrology, geochemistry and age relations of Triassic and Tertiary volcanic rocks from SW Egypt and NW Sudan. J. Afr. Earth. Sci. 6, 335–352.

Gaina, C., Roest, W.R., Muller, R.D., 2002. Late cretaceous–cenozoic of northeast Asia. Earth Planet. Sci. Lett. 197, 273–286. http://dx.doi.org/10.1016/s0012-821X(02)00499-5.

Ganerød, M., Smethurst, M.A., Rousse, S., Torsvik, T.H., Prestvik, T., 2008. Reassembling the paleogene–eocene North Atlantic igneous province: new paleomagnetic constraints from the Isle of Mull, Scotland. Earth Planet. Sci. Lett. 272, 464–475.

Ganerød, M., Smethurst, M.A., Torsvik, T.H., Prestvik, T., Rousse, S., McKenna, C., van Hinsbergen, D.J.J., Hendriks, B.W.H., 2010. The North Atlantic igneous province reconstructed and its relation to the Plume Generation Zone: the Antrim Lava Group revisited. Geophys. J. Int. 182, 183–202.

Gradstein, F., Ogg, J., Schmitz, M., Ogg, G., 2012. The geologic time scale 2012, 1st ed. Elsevier, Boston, USA. http://dx.doi.org/10.1016/B978-0-444-59425-9.00004-4.

Hodgson, B.D., Dagley, P., Mussett, A.E., 1990. Magnetostratigraphy of the Tertiary igneous rocks of Arran. Scott. J. Geol. 26, 99–118.

Issawi, B., El Hinnawi, M., Francis, M., Mazhar, A., 1999. The Phanerozoic Geology of Egypt: A geodynamic Approach. The Egyptian Geological Survey, special publication 76.

Jacobson, D., Beck, M.E., Diehl, J.F., Hearn, B.C., 1980. A Paleocene paleomagnetic pole of North America from alkali intrusions, central Montana. Geophys, Res, Lett 7, 549–552.

Kirschvink, J.L., 1980. The least squares line and plane and the analysis of paleomagnetic data. Geophys. J. R. Astr. Soc. 62, 699–718.

Klitzsch, E., 1984. Northwestern Sudan and bordering areas: geological development since Cambrian time. Berliner Geow. Abh. A 50, 23–45.

Klitzsch, E., Lejal-Nicol, A., 1984. Flora and fauna from strata in Southern Egypt and Northern Sudan (Nubia and surrounding areas). Berliner Geowiss. Abh. A 50, 47–79.

Klitzsch, E., List, F.K., Pöhlmann, G., Handley, R., Hermina, M., Meissner, B., (Eds.) (1986–1987) Geological map of Egypt, 1:500 000, Bir Misaha Sheet [NF35NE]. Cairo: Conoco Coral, the Egyptian Petroleum Corporation, Egypt.

Lerbeckmo, J.F., Coulter, K.C., 1985. Late Cretaceous to early Tertiary magnetostratigraphy of a continental sequence: Red Deer Valley, Alberta, Canada. Canad. J. Earth Sci. 22, 567–583.

Lotfy, H.I., 2011. Active concomitant counterclockwise rotation and northwards translation of Africa during the Mid- late cretaceous: a paleomagnetic study on the Wadi Natash alkaline volcanic province (104–84 Ma), South Eastern Desert, Egypt. Palaeogeog. Palaeoclim. Palaeoecol. 310, 176–190.

Lotfy, H.I., 2015. Early Cretaceous counterclockwise rotation of Northeast Africa within the equatorial zone: Paleomagnetic study on Mansouri ring complex, Southeastern Desert, Egypt. NRIAG J. Astronomy Geophys. 4 (1), 1–15. http://dx.doi.org/10.1016/j.nrjag.2015.01.001.

McElhinny, M.W., Lock, J., 1996. IAGA paleomagnetic databases with access. Surv. Geophys. 17 (5), 575–591, doi: 19.1038/2161276a0.

McFadden, P.L., Lowes, F.J., 1981. The discrimination of mean directions drawn from Fisher distributions. Geophys. J. R. Astr. Soc. 67, 19–33.

McMahon, B.E., Strangway, D.W., 1968. Investigation of Kiaman Magnetic Division. Gephys. J. Roy. Astron. Soc. 15, 265–285.

Müller, R.D., Roest, W.R., Royer, J.-Y., Gahagan, L.M., Sclater, J.G., 1997. Digital isochrones of the world's ocean floor. J. Geophys. Res. 102, 3211–3214. http://dx.doi.org/10.1029/96JB01781.

Nürnberg, D., Müller, R.D., 1991. The tectonic evolution of the South Atlantic from Late Jurassic to present. Tectonophysics 191, 27–53.

Pisarevsky, S.A., 2005. New edition of the Global Paleomagnetic Database. EOS 86 (17), 170.

Riisager, P., Riisager, J., Abrahamsen, N., Waagstein, R., 2002. New paleomagnetic pole and magnetostratigraphy of Faroe Islands flood volcanics, North Atlantic Igneous Province. Earth Planet. Sci. Lett. 201, 261–276.

Riisager, J., Riisager, P., Pedersen, A.K., 2003a. The C27n-C26r geomagnetic polarity reversal recorded in the West Greenland flood basalt province: how complex is the transitional field? J. Geophys. Res. 108, 2155. http://dx.doi.org/10.1029/2002JB002124.

Riisager, J., Riisager, P., Pedersen, A.K., 2003b. Paleomagnetism of large igneous province: case-study from West Greenland, North Atlantic igneous province. Earth Sci. Planet. Lett. 214, 409–425.

Robertson, A.H.F., Grasso, M., 1995. Overview if the Late Tertiary-recent tectonic and palaeo-environmental development of the Mediterranean region. Terra Nova 7, 114–127.

Schandelmeier, H., Darbyshire, F., 1984. Metamorphic and magmatic events in the Uweinat- Bir Safsaf uplift (Western Desert, Egypt). Geol. Rundsch. 73, 819–831.

Schandelmeier, H., Richter, A., Franz, G., 1983. Outline of the geology of magmatic and metamorphic units from Gebel Uweinat to Bir Safsaf (SW Egypt/ NW Sudan). J. Afr. Earth Sci. 1, 275–283.

Schandelmeier, H., Huth, A., Harms, U., Franz, G., Berneau, R., 1987. The East Saharan Craton in Southern Egypt and Northern Sudan: lithology, metamorphism, magmatism, geochronology and structural development. Berliner Geow. Abh. A 75, 5–48.

Schwarz, E.J., Coleman, L.C., Cattroll, H.M., 1979. Paleomagnetic results from the Skaergaard intrusion, East Greenland. Earth Planet. Sci. Lett. 42, 437–443.

Tarling, D.H., 1967. Palaeomagnetic properties of some Tertiary lavas from East Greenland. Earth Sci. Planet. Lett. 3, 81–88.

Torsvik, T.H., Muller, R.D., Van der Voo, R., Steingerger, B., Gaina, C., 2008. Global plate motion frames: toward a unified model. Rev. Geophys. 46 (RG3004/2008), 1–44.

Torsvik, T.H., Van der Voo, R., Preeden, U., Mac Niocaill, C., Steinberger, B., Doubrovine, P., van Hinsbergen, D.J.J., Domeier, M., Gaina, C., Tohver, E., Meert, J.G., McCausland, P.J.A., Cocks, L.R.M., 2012. Phanerozoic polar wander. Paleogeogr. Dynamics. Earth-Sci. Rev. 114, 325–368.

Van der Voo, R., 1993. Paleomagnetism of the Atlantic, Tethys and Iapetus Oceans. Cambridge University Press, Cambridge, U.K.

Vugteveen, R.W., Barnes, A.E., Butler, R.F., 1981. Paleomagnetism of the Roskruge and Gringo Gulch Volcanics, Southeast Arizona. J. Geophys. Res. 86, 4021–4028.

Wilson, R.L., Ade-Hall, J.M., Skelhorn, R.R., Speight, J.M., Dagley, P., 1974. The British Tertiary Igneous Province: Palaeomagnetism of the Vaternish dyke swarm on North Skye, Scotland. Gephys. J. Roy. Astron. Soc. 37, 23–30.

Wilson, R.L., Hall, J.M., Dagley, P., 1982. The British Tertiary igneous province: palaeomagnetism of the dyke swarm along the coast of Skye. Geophys. J. Roy. Astron. Soc. 68, 317–323.

Zijderveld, J.D.A., 1967. A. C. demagnetization of rocks. In: Collinson, D.W., Creer, K.M., Runcorn, S.K. (Eds.), Methods in Paleomagnetism. Elsevier, New York, pp. 256–286.